

Effects of Particle Size and Rubber Content on Fracture Toughness in Rubber-Modified Epoxies

D. S. KIM,* K. CHO, J. K. KIM, and C. E. PARK**

Department of Chemical Engineering
Pohang University of Science and Technology
Pohang 790-784, Korea

The effects of particle size of core-shell rubber on the fracture toughness of rubber-modified epoxies were investigated. Various sizes of core-shell rubber particles, from 0.16 to 1.2 μm in diameter, were synthesized by seeded emulsion polymerization. Particle size effects were clearly seen for lower crosslinked diglycidyl ether of bisphenol A (DGEBA)/piperidine resin. Fracture toughness increased as the particle size of core-shell rubber decreased from 1.2 to 0.4 μm . On the other hand, fracture toughness was constant in this range of particle sizes for higher crosslinked DGEBA/diaminodiphenylmethane (DDM) resin. Cavitation in the rubbery core and shear deformation in the matrix are the toughening mechanisms for DGEBA/piperidine resin, whereas cavitation is the only mechanism for DGEBA/DDM resin. Toughening effectiveness decreased with $<0.2 \mu\text{m}$ core-shell rubber particles since they are difficult to cavitate. The effects of core-shell rubber content on fracture toughness of rubber-modified epoxies were also examined. The optimum rubber content for maximum toughness of rubber-modified epoxies decreased with decreased particle size of core-shell rubber in shear deformable DGEBA/piperidine resin. But the fracture toughness of rubber-modified DGEBA/DDM resins increased as the rubber content increased.

INTRODUCTION

Particle size is known to be the important parameter affecting the fracture toughness of rubber-modified epoxies. Sultan and McGarry (1) were the first to show that rubber particle size influences the fracture toughness of rubber-modified epoxies. They showed that 40 nm particles are not as efficient as 1.2 μm particles in toughening, and inferred that crazing induced by larger particles of $\sim 1 \mu\text{m}$ absorbed more energy than shear yielding induced by smaller particles of a few hundred angstroms. Kunz-Douglas *et al.* (2) reported that smaller particles were more effective than larger particles, because of the tearing energy of rubber particle increase with size decrease. Margolina and Wu (3, 4) observed that brittle-ductile transition occurs at the critical inter-particle distance for materials toughened by shear yielding. This suggests that smaller particles are better toughening agents. Pearson and Yee (5) showed that smaller particles provide a significant increase in toughness by cavitation-induced shear bands, whereas large particles provide

only a modest increase in fracture toughness by a particle bridging/crack deflection mechanism. According to Pearson and Yee, larger particles cannot be cavitated, because they lie outside the plastic zone, proposed by Irwin (6), where the large hydrostatic stress exists. Lazzeri and Bucknall (7) have proposed a model for rubber particle cavitation showing that cavitation in the rubber particles cannot be formed by particles $<0.25 \mu\text{m}$ in diameter.

Particle size cannot be adjusted independently without changing other parameters such as properties of rubber particles, volume content of rubber particles, and adhesion strength between the matrix and the rubber particles since reactive liquid rubbers are incorporated in the epoxy resin matrix and form spherical particles during cure. Therefore, synthesized core-shell rubber particles were used here as a toughening agent for investigating the effects of rubber particle size on the fracture toughness of rubber-modified epoxies.

Volume content effects were also examined with the same size core-shell rubber particles. Michler (8) claimed that maximum fracture toughness is obtained only if the average inter-particle distance is between the critical minimum inter-particle distance and the critical maximum inter-particle distance. He

* Present address: Sunkyoung Industry, Corporate R&D Center, 600 Jungja-1-dong, Changan-ku, Suwon 440-745, Korea.

** To whom correspondence should be addressed.

Table 1. Recipes of Core and Core-Shell Rubber Particles in Emulsion Polymerization.*

	core 1	core 2	core 3	core 4	Ecore 1	CS(60/40) 1	CS(60/40) 2	CS(60/40) 3	CS(60/40) 4	CS(20/80) 1	ECS(20/80) 1	PMMA Shell
core 1 (g)	—	219.8	109.9	—	—	109.7	—	—	—	37.1	—	—
core 2 (g)	—	—	—	—	—	—	105.6	—	—	—	—	—
core 3 (g)	—	—	—	135.7	—	—	—	81.4	—	—	—	—
core 4 (g)	—	—	—	—	—	—	—	—	104.7	—	—	—
Ecore 1 (g)	—	—	—	—	—	—	—	—	—	—	112.6	—
BA (g)	150	80	140	50	250	—	—	—	—	—	—	—
MMA (g)	—	—	—	—	—	13.2	13.2	9.9	13.2	26.4	125.22	69.3
BDDM (g)	—	—	—	—	—	0.13	0.13	0.1	0.13	0.26	1.25	0.69
SLS (g)	—	—	—	—	1.03	—	—	—	—	—	1.97	—
KPS (g)	0.90	0.48	0.84	0.3	0.83	0.08	0.08	0.06	0.08	0.16	1.80	0.42
water (g)	600	300	550	189	636	700	700	534	715	770	550	630
solid conc. (%)	18.2	18.9	18.4	19.1	27.4	3.9	3.6	3.6	3.5	3.9	19	9.8

* Polymerization temperature: 70°C, atmosphere: N₂, and reaction time: 6 hr.

Table 2. Size and T_g of Core and Core-Shell Rubber Particles.

	core 1	core 2	core 3	core 4	Ecore 1	CS(60/40) 1	CS(60/40) 2	CS(60/40) 3	CS(60/40) 4	CS(20/80) 1	ECS(20/80) 1	PMMA Shell
T _g (°C) core	-49	-50	-50	-49	-48	-52	-53	-53	-50	-51	-50	—
shell	—	—	—	—	—	120	119	120	116	120	124	123
diameter** (μm)	0.34	0.51	0.75	1.03	0.10	0.40	0.60	0.90	1.20	0.56	0.16	0.35

* T_g's were measured by DSC with scanning rate of 10°C/min.

** Diameters of core-shell rubber particles were measured from SEM micrographs and those of core particles were calculated from the diameters of core-shell rubber particles and weight fractions of cores.

explained that stress concentration is smeared over a larger volume as a consequence of the existence of entangled and interconnected macromolecules with less than the critical minimum inter-particle distance, and the transition from plane strain to plane stress cannot occur with larger than the critical maximum inter-particle distance.

Many have reported (9–11) that the combination of rubber cavitation and shear deformation of matrix is the major toughening mechanism in rubber-modified epoxies. The “toughenability” of rubber-modified thermosets depends upon the crosslink density of the matrix since the amount of shear deformation decreases as the crosslink density increases (12, 13). The effects of the crosslink density of epoxy resins are also explored here by varying the particle size and the volume content of core-shell rubber particles.

EXPERIMENTAL

Materials

The epoxy resin used was YD-128 resin, which is diglycidyl ether of bisphenol-A (DGEBA) epoxy resin (Kukdo Chemical Co., equivalent epoxy weight: 187 ± 3). The curing agents used were piperidine (Junsei Chemical Co.) or diaminodiphenyl methane (DDM, Aldrich Chemical Co.) depending on the crosslink density of epoxy resins. As a toughening agent, core-shell rubber particles were synthesized using butyl acrylate (BA, Aldrich Chemical Co.) as a core rubber particle and methyl methacrylate (MMA, Junsei Chemical Co.) as a shell. BA and MMA were washed with 10% aqueous sodium hydroxide to remove the initiator before

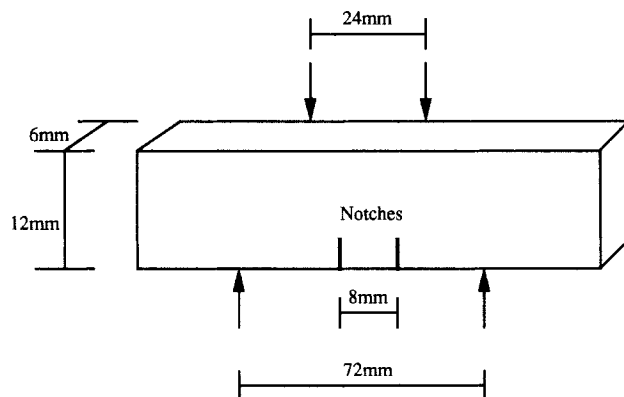


Fig. 1. Schematic diagram of the double-notched four-point bending (DN-4PB) test geometry.

use. An amount of 1.0 wt% of 1,4-butanediol dimethacrylate (BDDM, Aldrich Chemical Co.) was added as a crosslinking agent for MMA to prevent swelling of core-shell particles in the epoxy resin. Potassium persulfate (KPS, Junsei Chemical Co.) and sodium lauryl sulfate (SLS, Taedong Chemical Co.) were used as a redox initiator and an emulsifier for emulsion polymerization, respectively. Distilled-deionized water (resistance: 18MΩ) was used for emulsion polymerization.

Preparation of Core-Shell Particles

Table 1 shows the recipes of core and core-shell particles in emulsion polymerization. After an polybutylacrylate (PBA) emulsion core (core1) was made, big-

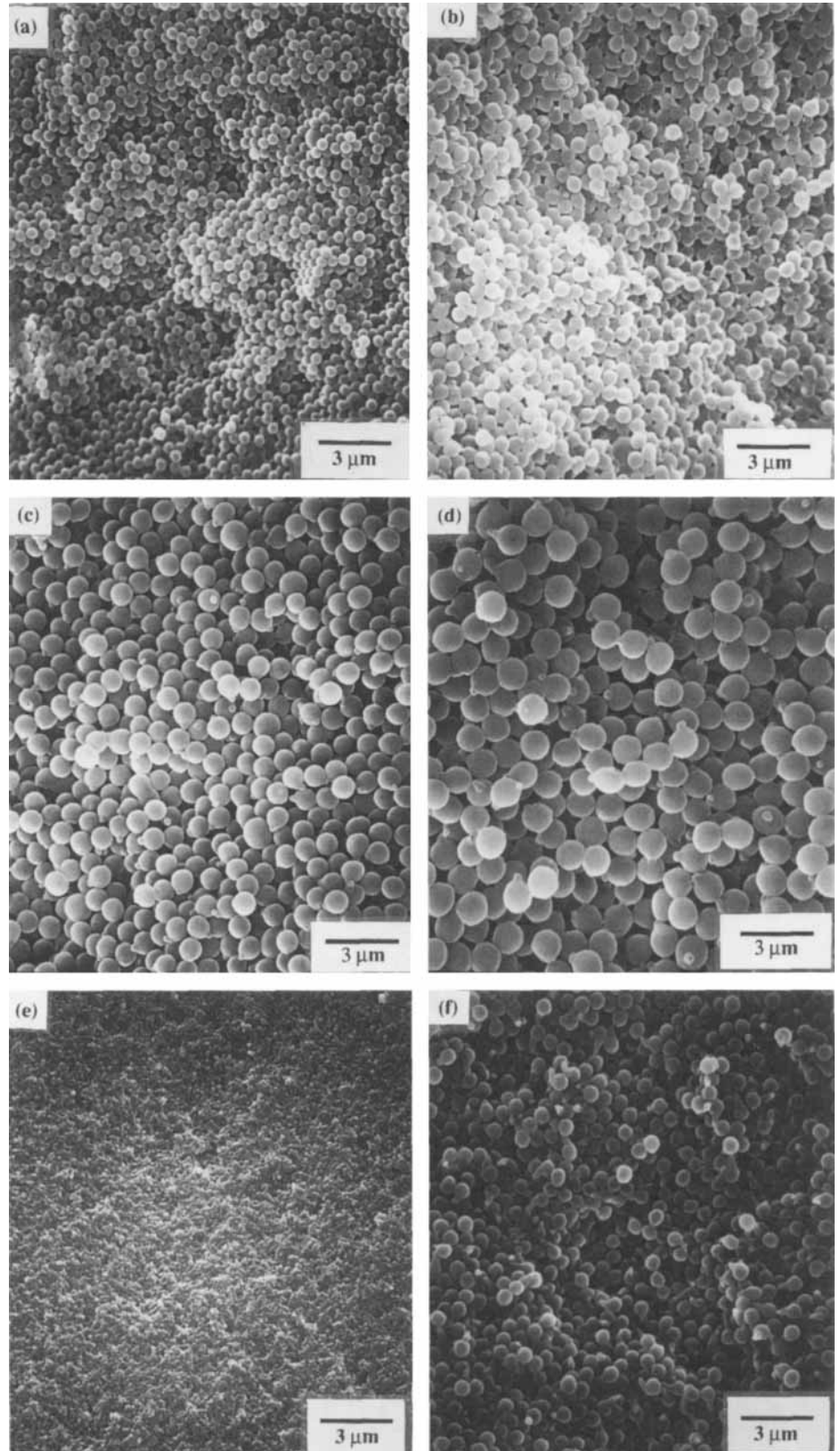


Fig. 2. SEM micrographs of core-shell rubber particles: (a) CS(60/40)1, (b) CS(60/40)2, (c) CS(60/40)3, (d) CS(60/40)4, (e) ECS(20/80)1, and (f) CS(20/80)1.

ger cores (core2, core3, and core4) were stepwise synthesized by emulsifier-free seeded emulsion polymerization. Then, the cores were encapsulated by emulsifier-free seeded emulsion polymerization of MMA to produce core-shell particles (CS1, CS2, CS3, and CS4). In this way, the core-shell particle size was varied from 0.4 μm to 1.2 μm (Table 2). Emulsifier was employed to make a 0.1 μm core (Ecore1) and a 0.16 μm core-shell particle (ECS1). The ratios of core to shell were 60/40 (wt/wt) for larger than 0.4 μm core-

shell particles, and 20/80 (wt/wt) for less than 0.2 μm core-shell particles. Since the ratio of surface area to the volume increases with decreasing particle size, the amount of shell has to be increased up to 80 wt% to prevent the coagulation of 0.16 μm core-shell particles. Throughout the paper, the ratio of core to shell is indicated in parenthesis in the notation of core-shell particles, for instance, CS(60/40)1. Emulsion polymerization was performed in a 1000 cm^3 resin kettle equipped with a condenser, mechanical stirrer, and

Fig. 3. SEM micrographs of fracture surfaces of 10 phr core-shell rubber-modified YD-128/piperidine resins fractured in liquid nitrogen: (a) CS(60/40)1, (b) CS(60/40)2, (c) CS(60/40)3, and (d) CS(60/40)4.

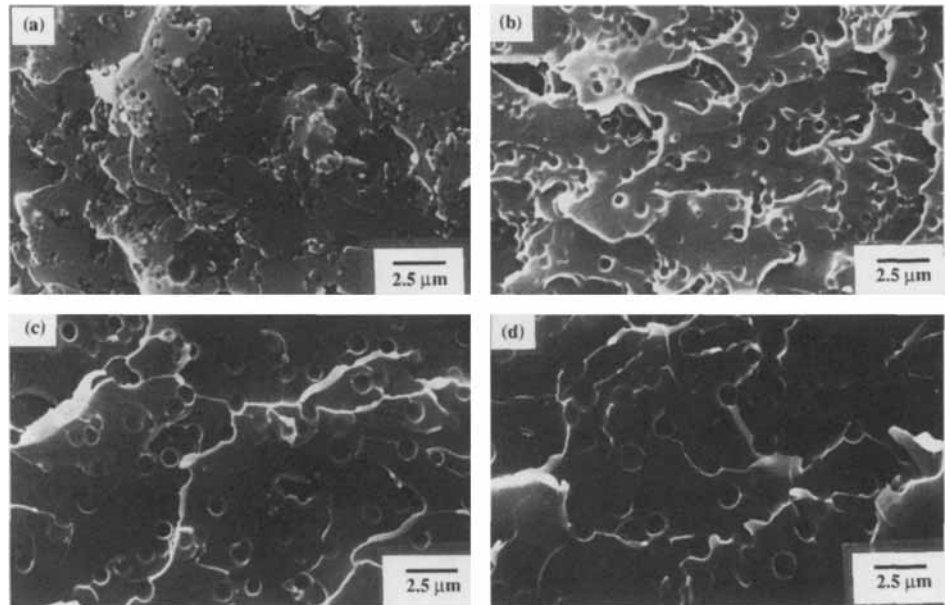


Table 3. Mechanical Properties of Core-Shell Rubber Modified YD-128/Piperidine Resins.

Formulation	Core-Shell Content (phr)	Surface-to-Surface Inter-Particle Distance (μm)	Fracture Toughness K_{IC} ($\text{MPa}\cdot\text{m}^{1/2}$)	Flexural Modulus (MPa)	Flexural Strength (MPa)	Flexural Strain at Break (%)
YD-128/Piperidine	—	—	0.88 ± 0.05	2986 ± 104	122.6 ± 4.2	5.66 ± 0.16
YD-128/Piperidine/Toughening Agents						
CS(60/40) 1	10	0.35	2.88 ± 0.04	2721 ± 57	104.7 ± 1.9	5.55 ± 0.26
CS(60/40) 2	10	0.52	2.63 ± 0.02	2707 ± 59	104.2 ± 1.9	5.56 ± 0.25
CS(60/40) 3	10	0.79	2.56 ± 0.03	2665 ± 75	104.7 ± 1.6	5.66 ± 0.21
CS(60/40) 4	10	1.06	2.19 ± 0.03	2674 ± 73	102.9 ± 0.8	5.61 ± 0.17
PMMA shell	10	—	1.03 ± 0.05	2863 ± 109	118.8 ± 1.2	5.66 ± 0.16
CTBN 1300X8	10	—	2.42 ± 0.04	2469 ± 22	101.2 ± 0.8	5.61 ± 0.61
CS(20/80) 1	10	0.68	2.02 ± 0.03	3103 ± 62	80.8 ± 5.2	2.71 ± 0.21
CS(60/40) 1	5	0.52	2.63 ± 0.03	2897 ± 39	109.1 ± 1.8	5.35 ± 0.14
	10	0.35	2.88 ± 0.04	2721 ± 57	104.7 ± 1.9	5.55 ± 0.26
	15	0.27	2.80 ± 0.06	2551 ± 41	88.1 ± 1.3	4.77 ± 0.44
	20	0.22	2.53 ± 0.11	2544 ± 24	78.3 ± 2.1	3.86 ± 0.08
	30	0.16	1.78 ± 0.15	2249 ± 62	56.2 ± 3.6	2.77 ± 0.26
CS(60/40) 3	5	1.19	2.29 ± 0.04	2792 ± 36	108.4 ± 3.0	5.28 ± 0.47
	10	0.79	2.56 ± 0.04	2665 ± 75	104.7 ± 1.6	5.66 ± 0.21
	20	0.50	2.76 ± 0.07	2400 ± 80	80.7 ± 5.2	3.99 ± 0.50
	30	0.36	2.49 ± 0.06	2200 ± 72	66.1 ± 3.4	3.49 ± 0.51
ECS(20/80) 1	5	0.26	1.68 ± 0.04	2968 ± 40	116.6 ± 1.1	5.28 ± 0.15
	10	0.19	2.03 ± 0.10	2944 ± 43	117.2 ± 2.7	5.26 ± 0.14
	15	0.15	1.86 ± 0.04	2934 ± 71	109.7 ± 3.2	4.59 ± 0.61
	20	0.13	1.82 ± 0.08	2868 ± 74	98.2 ± 5.8	3.86 ± 0.36
	30	0.10	1.11 ± 0.04	2916 ± 20	78.5 ± 8.3	2.79 ± 0.29

nitrogen inlet at a reaction temperature of 70°C and a stirring speed of 200 rpm.

Sample Preparation for Mechanical Tests

Powders of core-shell particles were obtained by filtering and vacuum drying at room temperature. The core-shell particles were mixed with the epoxy resin at room temperature. Then, the mixture was heated to 80°C and stirred for 1 h while degassing. After the slow addition of curing agent and stirring, the mixture was degassed and poured into preheated aluminum mold coated with polytetrafluoroethylene. The curing schedule for the neat and rubber-modified YD-128/piperidine resins with 5 parts per hundred resin (phr) of piperidine was 16 h at 120°C, and that for the neat and rubber-modified YD-128/DDM resins with 26 phr of DDM was 80°C for 2 h and 150°C for 2 h. After curing, the mold was allowed to cool to room temperature in the oven.

Fracture Toughness and Flexural Properties

Fracture toughness, K_{Ic} , was measured by a notched three-point-bending test according to ASTM E-399 with dimensions of $0.6 \times 1.2 \times 6.0$ cm. A sharp crack was introduced by careful tapping of a fresh razor blade, which had been immersed in liquid nitrogen, into the base of the saw cut. Crosshead speed was 0.5 mm/min.

Flexural properties such as flexural strength, flexural modulus, and flexural strain at break were measured by the three-point-bending test according to ASTM D-790 with dimensions of $0.3 \times 1.2 \times 6.0$ cm. Eight specimens per test were used to find fracture toughness and flexural properties. More details of fracture toughness and flexural properties are described elsewhere (14).

Microscopy

After the fracture test, the fracture surfaces were examined under a scanning electron microscope (SEM). Samples were sputtered with a gold on the fracture surface in order to avoid any charge buildup.

The mature process zone at the crack tip of the double-notched four-point bending (DN-4PB) specimen was examined under a transmitted optical microscope (OM) (5, 15). Figure 1 shows the geometry of DN-4PB specimen. There are two nearly identical sharp cracks cut into the same edge of the specimen with a fresh razor blade. The ratio between the crack spacing and the crack length must be greater than 0.75 in order to eliminate the interaction between the two cracks (16, 17). The specimens were tested at a crosshead speed of 0.5 mm/min. On loading of the specimen, one crack will propagate, but the other will not because the cracks cannot be precisely identical. Therefore, the stationary crack has the mature process zone at the crack tip. The thin sections are taken in the mid-plane (plane strain region) near the stationary crack of the fractured DN-4PB specimens, which are normal to the fractured surface and parallel to

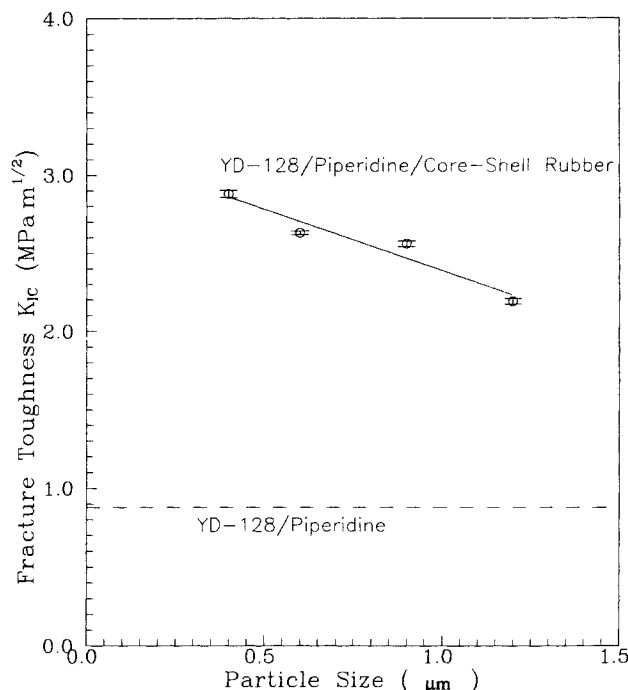


Fig. 4. Fracture toughness of 10 phr core-shell rubber modified YD-128/piperidine resins vs. particle size of core-shell rubber.

fracture direction. A petrographic polishing technique is employed to obtain thin sections of about 100 μm for transmitted OM (5, 18). These samples were examined using a Carl Zeiss Axioplan OM under bright field and crossed polarization.

Differential Scanning Calorimetry

A Perkin-Elmer DSC-7 was used to measure the glass transition temperatures (T_g) of the rubbery core and glassy shell. Measurements were performed on 10 mg samples using a scanning rate of 10°C/min. The T_g was defined as the temperature that corresponds to the midpoint of the observed heat capacity step-change for the glass transition.

Dynamic Mechanical Thermal Analysis

The T_g of the matrix and the modulus of the rubbery region ($T_g + 50^\circ\text{C}$) were determined using a dynamic mechanical thermal analyzer (DMTA, Polymer Laboratory). The dimensions of the specimen were 2.5 mm thickness, 7 mm width, and 20 mm length. The specimen was tested in a single cantilever mode and scanned at a frequency of 1 Hz from -80°C to 250°C with a heating rate of 3°C/min.

RESULTS AND DISCUSSION

Core-Shell Particles

As seen in scanning electron micrographs of core-shell particles (Fig. 2), every particle size is uniform. Table 2 shows that the glass transition temperatures of core and shell in core-shell particles measured by

Fig. 5. SEM micrographs of fracture surfaces of 10 phr core-shell rubber-modified YD-128/piperidine resins from notched three-point-bending tests: (a) CS(60/40)1, (b) CS(60/40)2, (c) CS(60/40)3, and (d) CS(60/40)4.

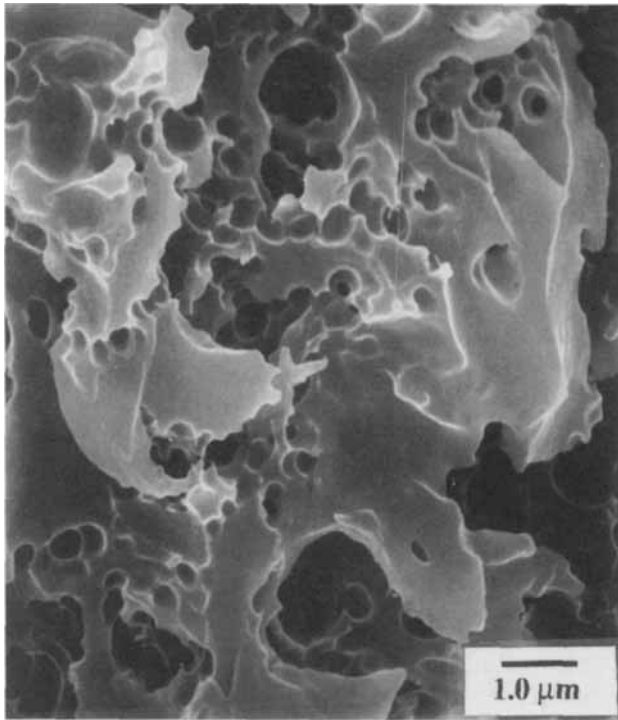
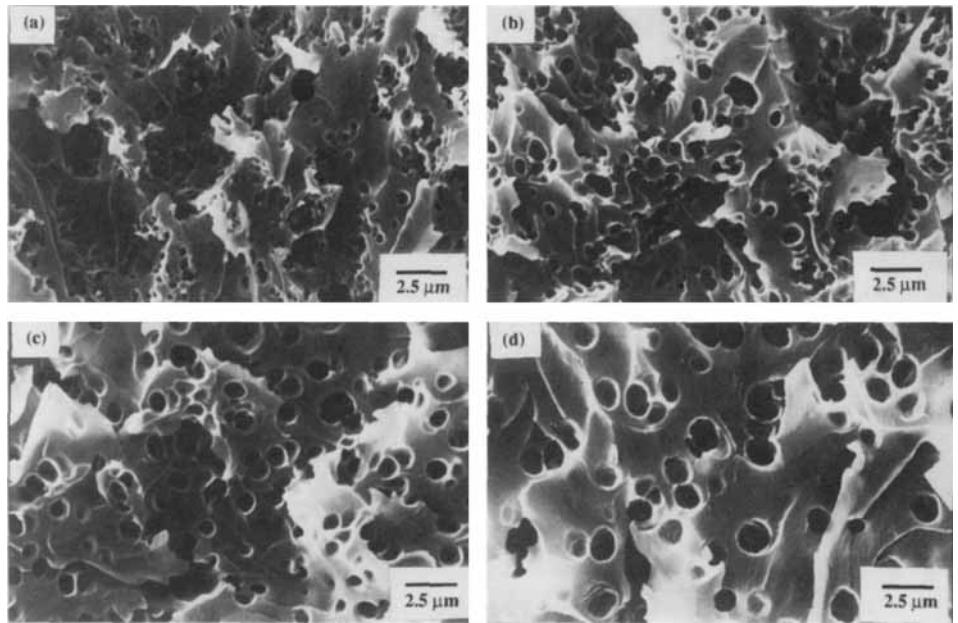


Fig. 6. SEM micrograph of fracture surface of 10 phr CS(60/40)1 modified YD-128/piperidine resin: higher magnification of Fig. 5a.

DSC are maintained at $-51 \pm 2^\circ\text{C}$ and $120 \pm 3^\circ\text{C}$, respectively, regardless of core-shell particle size, which indicates that the properties of the core-shell particles are the same. Diameters of core-shell particles measured from SEM micrographs were varied from 0.16 μm to 1.20 μm , and those of corresponding cores calculated from diameters of core-shell particles and weight fraction of cores were varied from 0.10 μm to 1.03 μm .

Crosslink Density of Epoxy Resins

Two different crosslink densities of YD-128 epoxy resins were obtained by using either piperidine or DDM as curing agents. Piperidine was used for lower crosslink density and DDM for higher crosslink density of epoxy resins. The effective crosslink density is related to molecular weight between crosslinks, which may be determined by use of an equation from the theory of rubber elasticity (19): $M_c = q\rho RT/G$, where M_c is the number average molecular weight between crosslinks, q is the front factor (usually equal to 1), ρ is the density at temperature T , T is the temperature (K), G is the equilibrium shear modulus in the rubbery region, and R is the gas constant. After measurement of the rubbery modulus (E) by DMTA, shear modulus was calculated by means of the equation $G = E/2(1 + \nu)$, where ν is the Poisson's ratio assumed as 0.35 (12, 20, 21). T_g obtained from DMTA was 100°C for YD-128/piperidine resin and 180°C for YD-128/DDM resin. Since the density at room temperature (1.193 g/cm^3 for YD-128/piperidine resin and 1.173 for YD-128/DDM resin) was used, a front factor q of 1 was employed to obtain reasonable values of M_c . The M_c was 1110 g/mol for YD-128/piperidine resin and 420 g/mol for YD-128/DDM resin. In this paper, the fracture toughness and the toughening mechanisms of core-shell rubber-particle-modified epoxy resins with quite different crosslink densities were investigated.

DGEBA (YD-128)/Piperidine

1. Effects of Particle Size

Figure 3 shows SEM micrographs of fracture surfaces of core-shell rubber-modified YD-128/piperidine resins fractured in liquid nitrogen. The size of embedded core-shell particles is the same as the core-shell emulsion, and the distribution is also uniform.

Fig. 7. Transmission optical micrographs of thin section taken mid-plane and near the crack tip of DN-4PB sample of 10 phr CS(60/40)1 rubber-modified YD-128/piperidine resin, viewed (a) in bright field and (b) using crossed-polarized light.

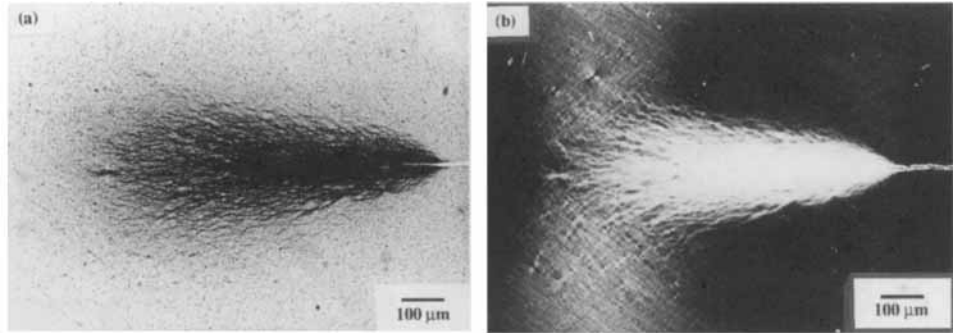


Fig. 8. Transmission optical micrographs of thin section taken mid-plane and near the crack tip of DN-4PB sample of 10 phr CS(60/40)4 rubber-modified YD-128/piperidine resin: (a) viewed in bright field, (b) higher magnification of (a), and (c) the same as (b) but viewed using crossed-polarized light.

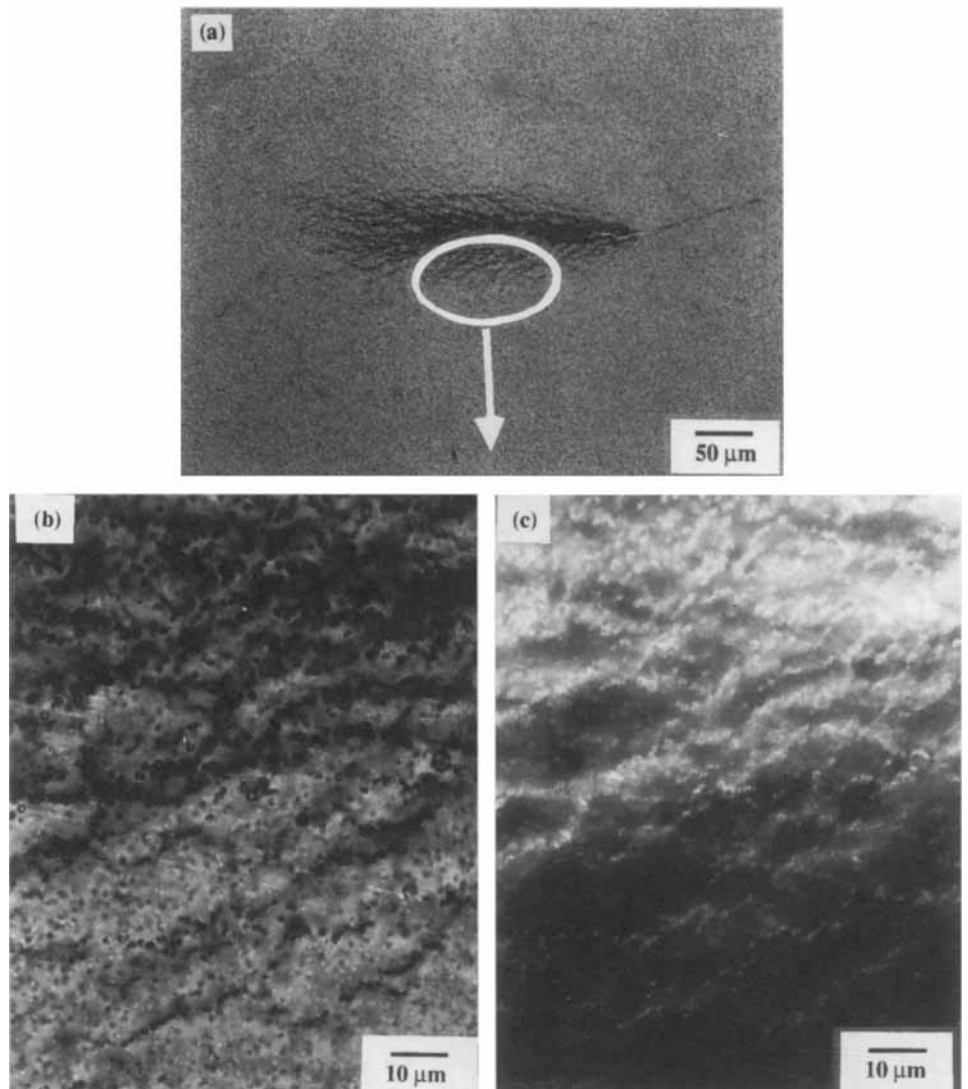


Table 3 shows fracture toughness and flexural properties of core-shell rubber-modified YD-128/piperidine resins. Flexural properties such as flexural modulus, flexural strength, and flexural strain at break were not changed with varying particle size, and decreased with increasing rubber content. Fracture toughness increased 3.3 times over that of neat epoxy resin with a decrease in core-shell particle size down

0.4 μm ; see Fig. 4. Fracture surfaces of core-shell rubber-modified YD-128/piperidine resins at the crack tip from notched three-point-bending tests (Fig. 5) show enlargement of core-shell particles and deformation of the matrix compared with those fractured in liquid nitrogen (Fig. 3). Cavitation in the rubbery core is clearly seen in Fig. 6, which is the high magnification SEM micrograph of CS(60/40)1 modified YD-

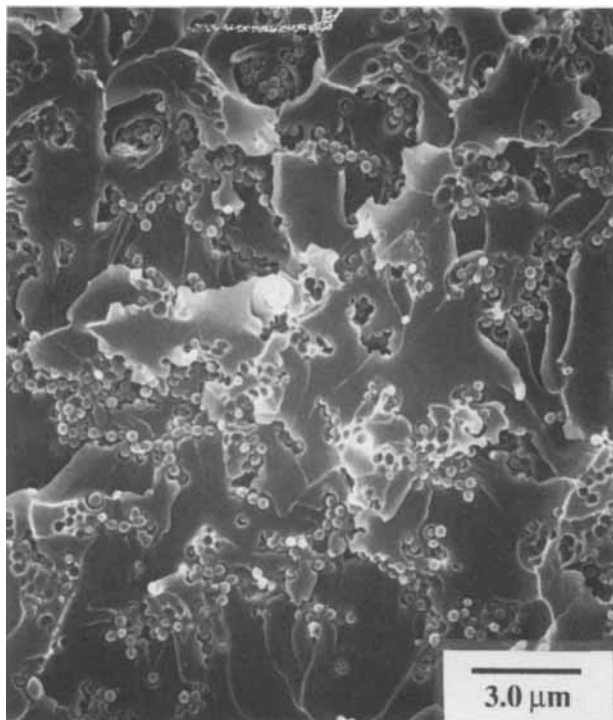


Fig. 9. SEM micrograph of fracture surface of 10 phr PMMA shell particle modified YD-128/piperidine resin.

128/piperidine resin. Figure 7 shows a transmission optical micrograph of a thin section taken in the mid-plane and near the crack tip of 10 phr CS(60/40)1 modified YD-128/piperidine resin, which had been tested using the double-notched four-point-bending method. In the bright field (Fig. 7a), a long dark elliptical zone, which is the stress-whitened zone in reflected light, is originated from light scattering by the cavities in the rubbery core. The process zone is darker in the middle and has lots of dark hairy lines around the boundary. In the crossed-polarized light (Fig. 7b), the dark region is converted to a white region. Figure 8 shows a transmission optical micrograph of a thin section taken in the mid-plane and near the crack tip of 10 phr CS(60/40)4 modified YD-128/piperidine resin. Cavitated particles appear black because of the scattering of visible light by the cavities, and are differentiated from other noncavitated white particles as shown in a higher-magnification micrograph (Fig. 8b). In the crossed-polarized light (Fig. 8c), white bands of birefringent material are seen to meander from particle to particle, which is characteristic of shear bands. It appears that the dark region in the bright field and the white region in the crossed-polarized light near the crack tip come from the high density of cavitated particles and the highly birefringent bands due to the sheared materials.

The increase of fracture toughness for YD-128/piperidine resin modified with 10 phr 0.35 μm poly(methyl methacrylate) (PMMA) shell crosslinked using 1 wt% BDDM is only 1.2 times that of neat epoxy resin. The toughening mechanism of PMMA shell

modified YD-128/piperidine resin is debonding, as shown in Fig. 9, instead of cavitation in the core for core-shell modified YD-128/piperidine resin. This indicates that the rubbery core in the core-shell particle has an important role in the toughening of epoxy resins.

Figure 10 shows transmission optical micrographs of core-shell rubber or PMMA shell modified YD-128/piperidine resins with the same crack length viewed in the bright field and using crossed-polarized light. The size and thickness of the dark and white zones decreased with an increase in the size of core-shell particles, and a process zone was not seen with PMMA shell modified YD-128/piperidine resin. As the particle size of core-shell rubber decreases, the number of cavities in the rubbery core increases, owing to the increased number of core-shell particles, and shear band formation between the cavitated particles is much easier since a stress field can be superimposed with shorter inter-particle distances and transition from plane strain to plane stress can occur.

2. Effects of Volume Content

The effects of the volume content of core-shell rubber on the fracture toughness of core-shell rubber-modified YD-128/piperidine resins were investigated as shown in Table 3. Maximum toughness was obtained with ~ 10 and 20 phr core-shell rubber in CS(60/40)1 and CS(60/40)3 modified YD-128/piperidine resins, respectively. This means that the optimum rubber content for achieving the maximum fracture toughness decreases with a decrease in the size of core-shell particles. Figure 11 shows transmission optical micrographs of a thin section taken in the mid-plane and near the crack tip of CS(60/40)3 modified YD-128/piperidine resin with the same crack length in the bright field. The size of the deformation zone is the greatest with 20 phr core-shell content, and a shallow deformation zone along the crack line is observed with 30 phr core-shell rubber content, which is consistent with the fracture toughness results shown in Table 3. These experimental results coincide with those of Michler on high-impact polyamides and polypropylene (8). Michler has insisted that the distance between particles is decisive for obtaining the maximum fracture toughness when shear deformation prevails. Since there is an interrelation between particle diameter D and distance between particles A in accordance with

$$A = \left(3 \sqrt{\frac{\pi}{6V_p}} - 1 \right) \cdot D \quad (1)$$

where V_p is the particle volume content, inter-particle distance can be calculated from the known particle diameter and volume fraction. According to Michler, there is a window between the critical distance A_{\min} and A_{\max} between particles exhibiting the maximum fracture toughness. With less than the critical distance A_{\min} , a viscoelastic "smearing" of the stress concentration prevents shear deformation, and with larger than the critical distance A_{\max} , shear deformation cannot occur since stress concentration is low

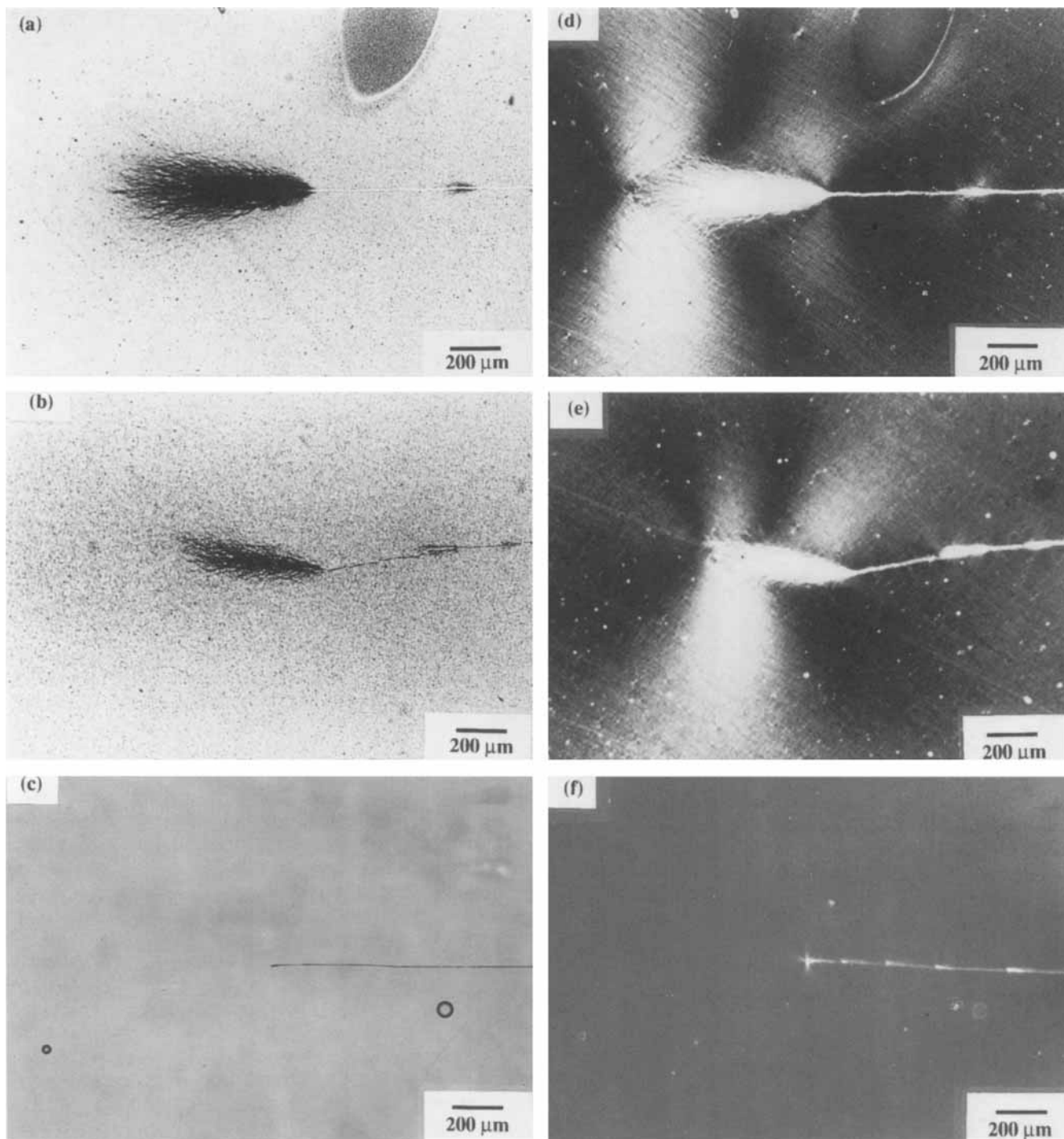


Fig. 10. Transmission optical micrographs of thin section taken mid-plane and near the crack tip of DN-4PB sample of 10 phr core-shell rubber-modified YD-128/piperidine resins, viewed in bright field: (a) CS(60/40)1, (b) CS(60/40)4, (c) PMMA shell, and using crossed-polarized light: (d) CS(60/40)1, (e) CS(60/40)4, (f) PMMA shell.

because of a lack of stress-field superposition. Michler reported that the window for polyamide is between ~ 100 and 300 nm. Judging from our experimental results (Fig. 12), the window for YD-128/piperidine resin appears to be between 300 and 600 nm. When the critical inter-particle distance was calculated using Eq. 1, the core diameter was employed as the particle diameter.

Less Than $0.2 \mu\text{m}$ Core-shell Rubber Particle

Figure 13 shows scanning electron micrographs of fracture surfaces of the stress-whitened region of ECS(20/80)1 modified YD-128/piperidine resins. The dispersibility of the core-shell particles in the matrix was poor with 5 phr ECS(20/80)1 particles (Fig. 13a). However, with more than 5 phr ECS(20/80)1 parti-

Fig. 11. Transmission optical micrographs of thin section taken mid-plane and near the crack tip of DN-4PB sample of (a) 5 phr, (b) 10 phr, (c) 20 phr, (d) 30 phr of CS(60/40)3 modified YD-128/piperidine resins, viewed in bright field.

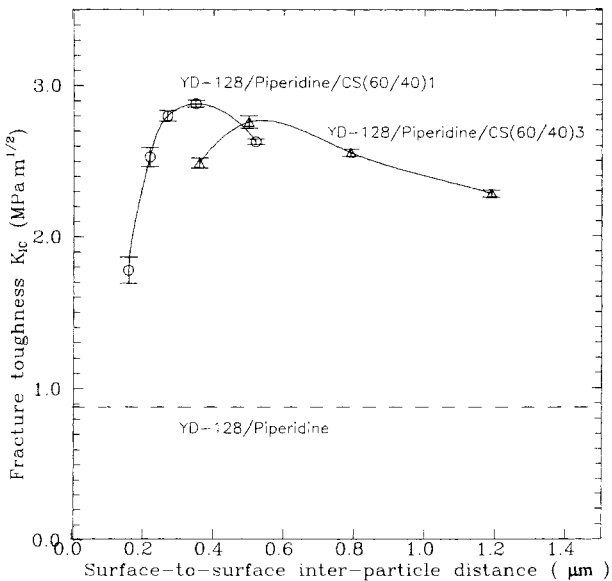
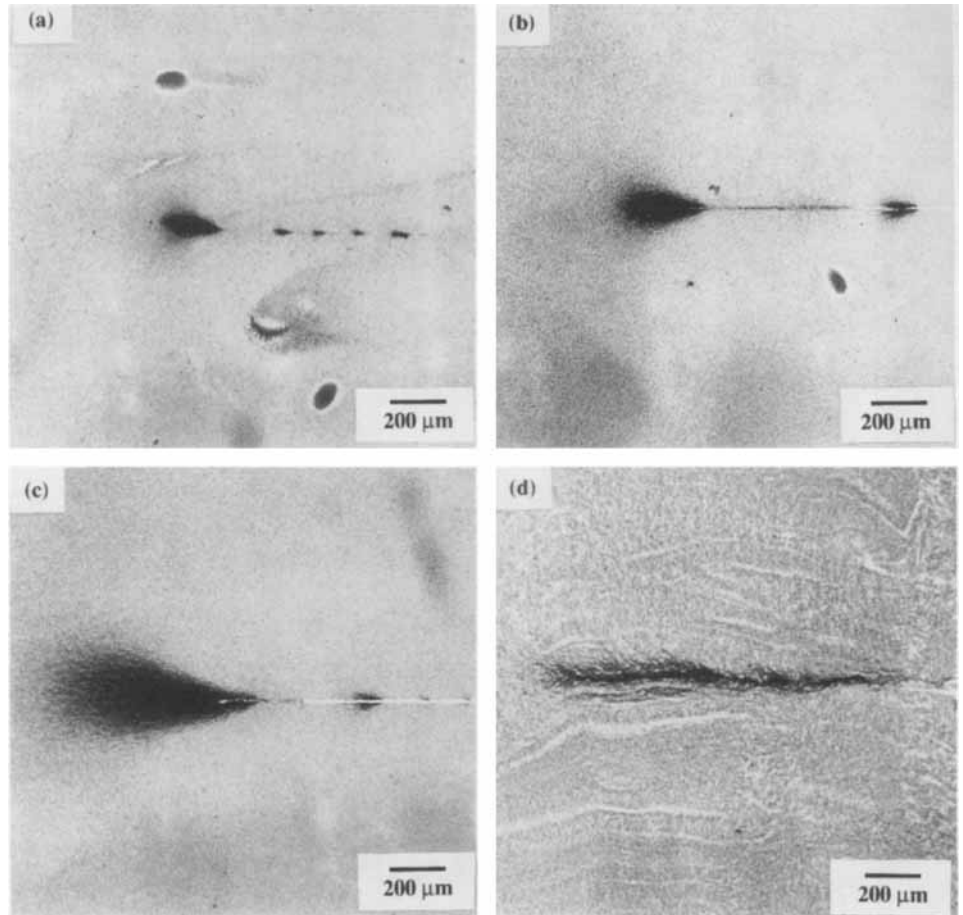


Fig. 12. Fracture toughness of core-shell rubber-modified YD-128/piperidine resins vs. surface-to-surface inter-particle distance.

cles, a uniform dispersion was obtained by mixing with a higher shear force. Since the viscosity of YD-128/piperidine resin and ECS(20/80)1 mixture increases with increased ECS(20/80)1 content, a high

shear force was required for uniform mixing. Since the core-shell particles with the same core and shell thickness synthesized without emulsifier can disperse uniformly in the matrix, the poor dispersion must be caused by the emulsifier used for emulsion polymerization.

The fracture toughness of ECS(20/80)1 modified YD-128/piperidine resins is lower than that of CS(60/40) modified ones. As seen in Fig. 13, debonding of the particles from the matrix is clearly evident, and cavitation in the rubbery core is hardly detected. It appears that debonding and little cavitation of ECS(20/80)1 modified YD-128/piperidine resin come from the small core-shell rubber particles. Gaymans *et al.* (22) have reported that rubber particles less than 0.2 μm appear to be very difficult to cavitate. Recently, Lazzeri and Bucknall (7) proposed that cavitation cannot be found in less than 0.25 μm rubber particles from the model study. For 0.16 μm ECS(20/80)1 modified YD-128/piperidine resins, debonding, a limited amount of cavitation, and shear deformation seem to be toughening mechanisms. The decrease of flexural modulus of ECS(20/80)1 modified samples is much less than that of CS(60/40) modified samples because of the smaller amount of rubber incorporated. It appears that the emulsifier does not affect the toughening mechanisms, since 0.4 μm ECS(60/40) modified samples show cavitation in the rubbery core.

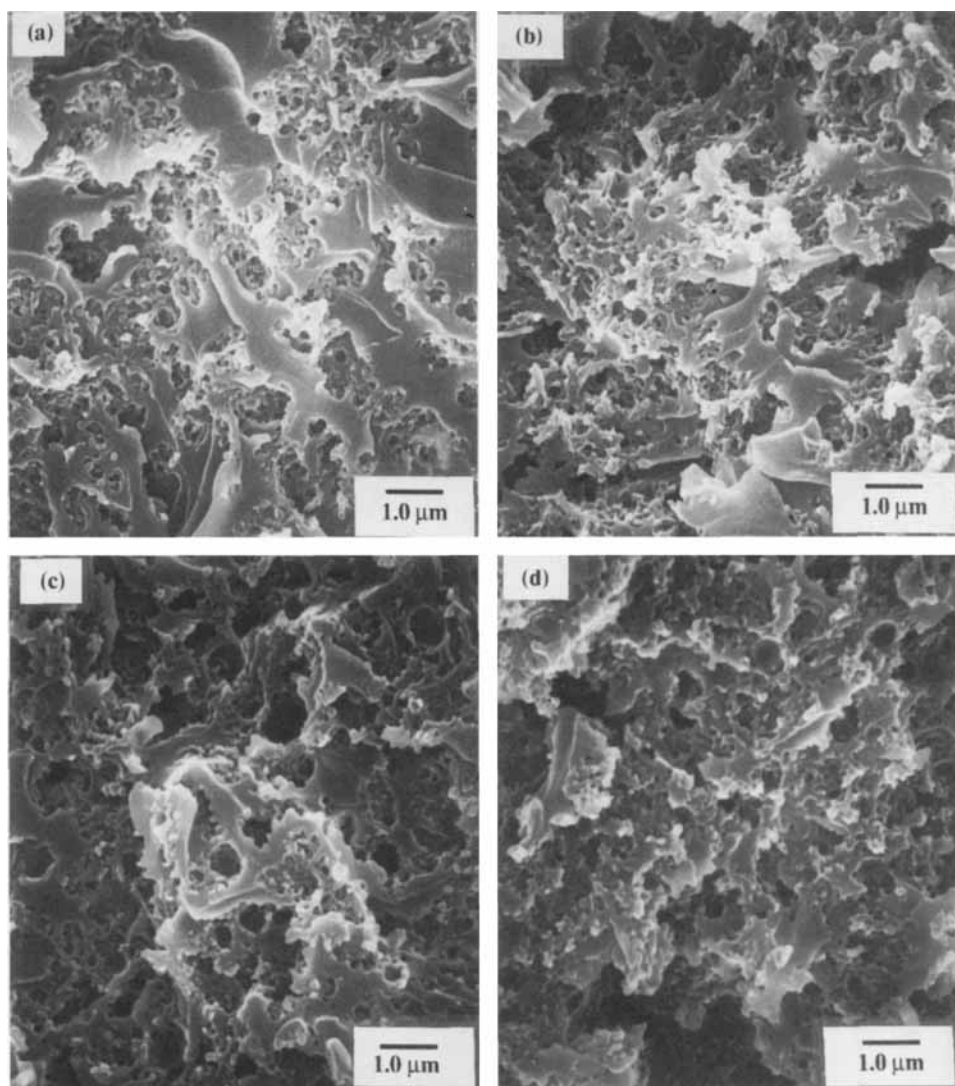


Fig. 13. SEM micrographs of fracture surfaces of (a) 5 phr, (b) 10 phr, (c) 20 phr, (d) 30 phr of ECS(20/80)1 modified YD-128/piperidine resins.

DGEBA (YD-128)/DDM

Table 4 shows the fracture toughness and flexural properties of CS(60/40) modified YD-128/DDM resins. Flexural properties such as flexural modulus,

flexural strength, and flexural strain at break decreased with increased core-shell rubber content. The fracture toughness of 10 phr CS(60/40) modified YD-128/DDM resins increased up to 1.2 times that of the

Table 4. Mechanical Properties of Core-Shell Rubber Modified YD-128/DDM Resins.

Formulation	Core-Shell Content (phr)	Surface-to-Surface Inter-Particle Distance (μm)	Fracture Toughness K_{Ic} ($\text{MPa}\cdot\text{m}^{1/2}$)	Flexural Modulus (MPa)	Flexural Strength (MPa)	Flexural Strain at Break (%)
YD-128/DDM	—	—	0.93 ± 0.05	2439 ± 58	142.3 ± 1.7	8.15 ± 0.41
YD-128/DDM/ Toughening Agents						
CS(60/40) 1	10	0.35	1.09 ± 0.03	2370 ± 150	99.1 ± 9.8	4.50 ± 0.69
CS(60/40) 2	10	0.52	1.10 ± 0.04	2178 ± 85	88.8 ± 12.4	4.32 ± 0.84
CS(60/40) 3	10	0.79	1.15 ± 0.02	2200 ± 103	95.6 ± 12.4	4.66 ± 0.89
CS(60/40) 4	10	1.06	1.14 ± 0.04	2192 ± 57	110.7 ± 11.7	6.28 ± 1.77
PMMA shell	10	—	1.05 ± 0.06	2512 ± 58	83.6 ± 7.7	3.49 ± 0.04
CS(60/40) 1	10	0.35	1.09 ± 0.03	2370 ± 150	99.1 ± 9.8	4.50 ± 0.69
	20	0.22	1.19 ± 0.06	2092 ± 74	76.6 ± 9.4	3.85 ± 0.61
	30	0.16	1.23 ± 0.07	1903 ± 98	61.7 ± 7.9	3.46 ± 0.62

neat resin, and independent of the size of CS(60/40) core-shell rubber particles, which is different from the YD-128/piperidine system. The stress-whitened zone in the fractured notched three-point-bending specimen was just a single line with the YD-128/DDM system. On the other hand, a thick stress-whitened zone was observed with the YD-128/piperidine system. Since the stress-whitened zone is formed by scattered light in the cavitated and debonded particles, the size of the stress-whitened zone is directly related to the fracture toughness, which coincides with the fracture toughness results.

Figure 14 shows scanning electron micrographs of stress-whitened zones of CS(60/40) modified YD-128/DDM resins. Compared with those of CS(60/40) modified YD-128/piperidine resins, shear deformation of the matrix and enlargement and deformation of core-shell particles were not observed, but cavitation in the rubbery core was noticed. Figure 15 shows transmission optical micrographs of thin sections in the midplane and near the crack tip of CS(60/40) modified YD-128/DDM resins in the bright field. A

circular process zone is seen in front of the crack tip, which comes from the cavitation in the rubbery core. Instead of cavitation, debonding is clearly seen in PMMA shell modified YD-128/DDM resins, as shown in Fig. 16.

The fracture toughness of CS(60/40) modified YD-128/DDM resins increased up to 1.3 times that of neat resin with increasing core-shell rubber content up to 30 phr. Since shear deformation cannot be formed, because of high crosslink density, and cavitation in the rubbery core is only the toughening mechanism, the increase in toughness is very limited and proportional to the content of core-shell rubber.

CONCLUSIONS

The effects of rubber particle size on fracture toughness of rubber-modified epoxies were studied using synthesized core-shell rubber particles as a toughening agent. By employing core-shell rubber particles instead of reactive liquid rubbers, particle size effects can be separately investigated without changing the

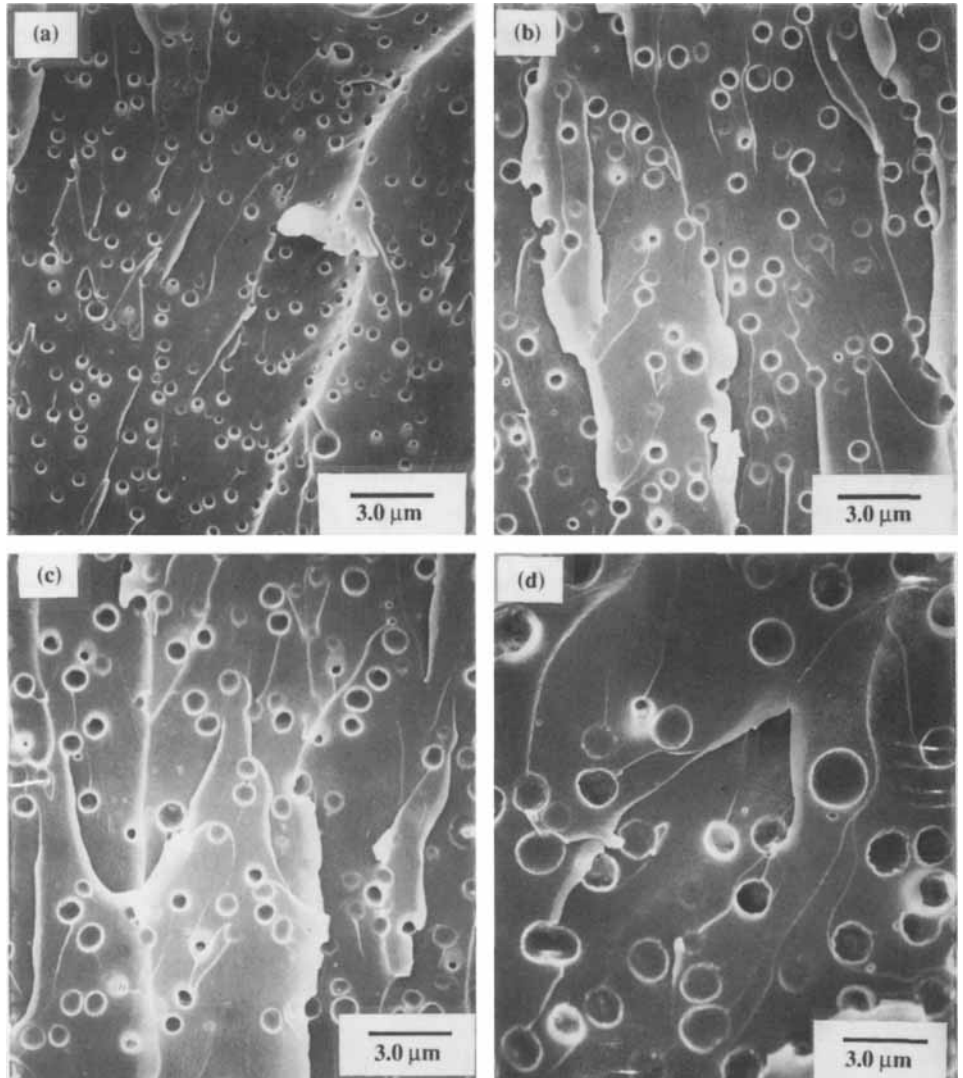


Fig. 14. SEM micrographs of fracture surfaces of 10 phr core-shell rubber-modified YD-128/DDM resins: (a) CS(60/40)1, (b) CS(60/40)2, (c) CS(60/40)3, and (d) CS(60/40)4.

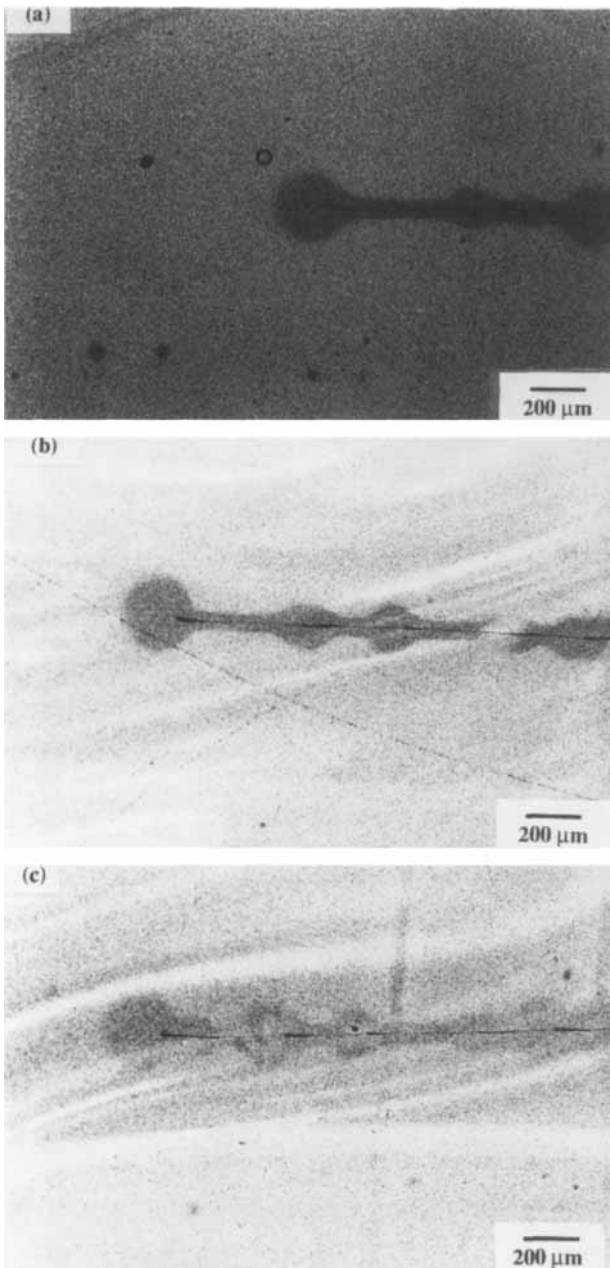


Fig. 15. Transmission optical micrographs of thin section taken mid-plane and near the crack tip of DN-4PB sample of 10 phr core-shell rubber modified YD-128/DDM resins, viewed in bright field: (a) CS(60/40)1, (b) CS(60/40)2, and (c) CS(60/40)3.

volume fraction of rubber particles, the properties of rubber particles, or the adhesion between matrix and rubber particles. For less crosslinked epoxy resins, the fracture toughness of rubber-modified epoxies increases as the core-shell particle size decreases. More shear deformation can be obtained with a smaller rubber particle size, since the stress field is superimposed owing to shorter inter-particle distances, and a transition from plane strain to plane stress occurs. But rubber particle size should be larger than $0.2 \mu\text{m}$ for effective toughening, since cavitation is difficult with

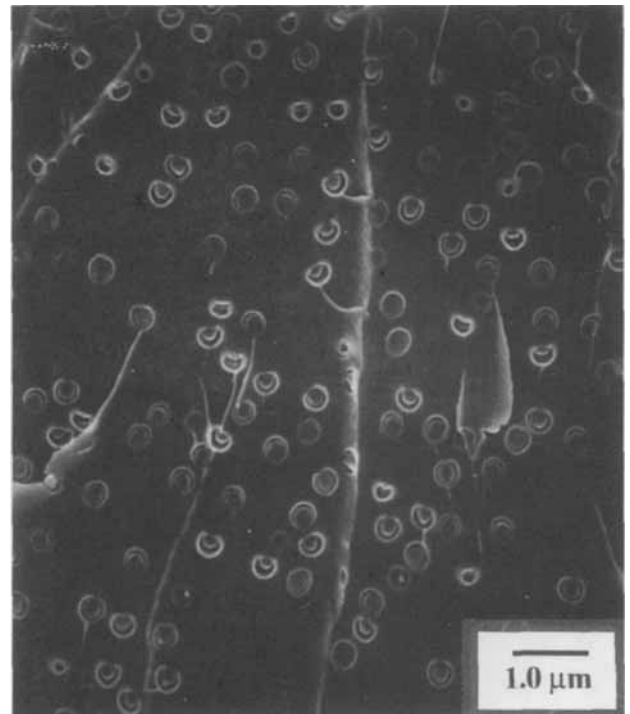


Fig. 16. SEM micrograph of fracture surface of 10 phr PMMA shell particle modified YD-128/DDM resin.

rubber particles less than $0.2 \mu\text{m}$. For highly crosslinked epoxy resins, rubber particle size effects were not observed since shear deformation cannot occur.

For less crosslinked epoxy resins, there is an optimum rubber content for maximum fracture toughness. The optimum rubber content decreases with decreased rubber particle size. It appears that there is a window for inter-particle distance to maximize fracture toughness: Shear deformation cannot form with larger than the critical inter-particle distance, and a viscoelastic smearing of the stress concentration prevents shear deformation with less than the critical inter-particle distance. For highly crosslinked epoxy resins, fracture toughness increases with increased rubber content since shear deformation cannot form and cavitation is the only energy absorbing mechanism.

ACKNOWLEDGMENT

This research was supported by the Korea Science and Engineering Foundation (Project number 90-04-00-09).

REFERENCES

1. J. N. Sultan and F. J. McGarry, *Polym. Eng. Sci.*, **13**, 29 (1973).
2. S. C. Kunz-Douglas, P. W. R. Beaumont, and M. F. Ashby, *J. Mater. Sci.*, **15**, 1109 (1980).
3. S. Wu, *Polymer*, **26**, 1855 (1985).
4. A. Margolina and S. Wu, *Polymer*, **29**, 2170 (1988).
5. R. A. Pearson and A. F. Yee, *J. Mater. Sci.*, **26**, 3828 (1991).
6. G. R. Irwin, *Appl. Mater. Res.*, **3**, 65 (1964).

7. A. Lazzeri and C. B. Bucknall, *J. Mater. Sci.*, **28**, 6799 (1993).
8. G. H. Michler, *Acta Polymer*, **44**, 113 (1993).
9. W. D. Bascom, R. Y. Ting, R. J. Moulton, C. K. Riew, and A. R. Siebert, *J. Mater. Sci.*, **16**, 2657 (1981).
10. A. J. Kinloch, S. J. Shaw, D. A. Tod, and D. L. Hunston, *Polymer*, **24**, 1341 (1983).
11. R. A. Pearson and A. F. Yee, *J. Mater. Sci.*, **21**, 2475 (1986).
12. A. J. Kinloch, C. A. Finch, and S. Hashemi, *Polym. Comm.*, **28**, 322 (1987).
13. R. A. Pearson and A. F. Yee, *J. Mater. Sci.*, **24**, 2571 (1989).
14. D. S. Kim, K. Cho, J. H. An, and C. E. Park, *J. Mater. Sci. Lett.*, **11**, 1197 (1992).
15. H. J. Sue, R. A. Pearson, D. S. Parker, J. Huang, and A. F. Yee, *Am. Chem. Soc. Polym. Preprints*, **30**, 147 (1988).
16. T. Kanazawa, S. Machida, S. Momoto, and Y. Hagiwara, in *Proc. 2nd International Conference on Fracture*, p. 1, Brighton, April 1969, P. L. Pratt, ed., Chapman and Hall, London (1969).
17. H. J. Sue, *Polym. Eng. Sci.*, **31**, 270 (1991).
18. A. S. Holik, R. P. Kambour, S. Y. Hobbs, and D. G. Fink, *Microstruct. Sci.*, **7**, 35 (1979).
19. J. D. Ferry, in *Viscoelastic Properties of Polymers*, 3rd Ed., Wiley, New York (1980).
20. Y. Hung and A. J. Kinloch, *Polymer*, **33**, 5338 (1992).
21. W. H. Lee, K. A. Hodd, and W. W. Wright, *J. Mater. Sci.*, **27**, 4582 (1992).
22. R. J. Gaymans, R. J. M. Borggreve, and A. J. Oostenbrink, *Makromol. Chem. Macromol. Symp.*, **38**, 125 (1990).